

STRUCTURE AND PROPERTIES OF NANOSCALE AND MESOSCOPIC MATERIALS

PACS numbers: 68.35.Ct, 68.37.Ef, 68.47.De, 68.47.Fg, 68.65.-k, 73.20.At, 81.16.Dn

Indium Deposited Nanosystem Formation on InSe (0001) Surface Applied as Template

P. V. Galiy, T. M. Nenchuk, A. Ciszewski*, P. Mazur*, Ya. M. Buzhuk,
Z. M. Lubun, and O. R. Dveriy**

*Ivan Franko National University of Lviv,
Electronics and Computer Technology Department,
1 Universytets'ka Str.,
UA-79000 Lviv, Ukraine*

**University of Wrocław, Institute of Experimental Physics,
9 Maxa Borna Plac,
50-204 Wrocław, Poland*

***Hetman Petro Sahaidachnyi National Army Academy,
Chair of Electromechanics and Electronics,
32 Heroes of Maidan Str.,
79026 Lviv, Ukraine*

Surface of two-dimensional InSe layered semiconductor crystal is applied as template for directed assembly of indium nanostructures. The study of In/(0001)InSe surface nanosystem formation is conducted using scanning tunnelling microscopy data. Indium is thermally deposited on structurally perfect InSe crystal cleavages obtained in ultra-high vacuum experimental conditions. It is able to achieve the formation of nanosized triangular shaped structures in a result of the solid state dewetting process by surface heating above the indium melting point. Moreover, the spatial arrangement of such nanostructures is powered by hexagonal lattice symmetry of InSe surface.

Key words: scanning tunnelling microscopy, low energy electron diffraction, layered crystals, indium selenide, nanostructures template directed assem-

Corresponding author: Pavlo Vasylyovych Galiy
E-mail: galiy@electronics.lnu.edu.ua

Citation: P. V. Galiy, T. M. Nenchuk, A. Ciszewski, P. Mazur, Ya. M. Buzhuk, Z. M. Lubun, and O. R. Dveriy, Indium Deposited Nanosystem Formation on InSe (0001) Surface Applied as Template, *Metallofiz. Noveishie Tekhnol.*, **41**, No. 10: 1395–1405 (2019), DOI: [10.15407/mfint.41.10.1395](https://doi.org/10.15407/mfint.41.10.1395).

bly, hetero-nanostructures.

Поверхня двовимірного шаруватого напівпровідникового кристала InSe використовувалася в якості шаблону для спрямованої збірки індієвих наноструктур. Дослідження наносистеми In/(0001)InSe проводилося за допомогою даних сканувальної тунельної мікроскопії. Індій наносили за допомогою методу термічного напилення на структурно досконалі поверхні сколювання кристалів InSe, отримані в експериментальних умовах надвисокого вакууму. Вдалося досягти формування точкових нанорозмірних структур трикутної форми внаслідок процесу повторного змочування поверхні твердого тіла внаслідок її нагріву вище температури плавлення індію. Крім того, просторове розташування таких наноструктур обумовлене гексагональною симетрією поверхневої ґратки кристалу InSe.

Ключові слова: сканувальна тунельна мікроскопія, дифракція повільних електронів, шаруватий кристал, селенід індію, спрямована шаблоном збірка наноструктур, гетеро-наноструктури.

Поверхность двумерного слоистого полупроводникового кристалла InSe использовалась в качестве матрицы для направленной сборки наноструктур индия. Исследование формирования наносистемы In/(0001)InSe проводилось с использованием данных сканирующей туннельной микроскопии. Индий термически напыляли на структурно совершенные поверхности скалывания кристаллов InSe, полученные в экспериментальных условиях сверхвысокого вакуума. Удалось добиться формирования точечных наноразмерных структур треугольной формы в результате процесса вторичного смачивания поверхности твёрдого тела вследствие её нагрева выше температуры плавления индия. Кроме того, пространственное расположение таких наноструктур обуславливается гексагональной симметрией поверхностной решётки InSe.

Ключевые слова: сканирующая туннельная микроскопия, дифракция медленных электронов, слоистый кристалл, селенид индия, направленная шаблоном сборка наноструктур, гетеро-наноструктуры.

(Received June 10, 2019)

1. INTRODUCTION

The covalent bonding in a layer with a different degree of iconicity and a weak van der Waals coupling between layers are inherent to the layered semiconductor crystals of In–Se system [1]. These features lead to the possibility of obtaining superfine 2D structures with semiconducting properties, ultimately monolayer in thickness, which are promising for nanoelectronics. Particularly, 2D layered semiconductor InSe is the object of modern research suitable for the functional nanoscale devices applications [2], for example, in the future super-fast electronics [3]. We previously reported on the valuable nanoscale properties of

Ni_xInSe hybrid metal-semiconductor system obtained as self-assembling system due to intercalation process [4]. A number of studies concerning the application of In₄Se₃ crystal were presented, such as In₄Se₃ based field effect transistor [5], thermoelectricity generation [6].

Due to intrinsic bulk anisotropy of layered crystals in In–Se system their surfaces: (0001) for hexagonal lattice InSe crystal polytype and (100) for In₄Se₃ crystal, might be just easily obtained juvenile by cleavage even in UHV which makes them suitable for use as a template for obtaining nanosystems *in situ*. There are a number of methods for obtaining metallic nanowires and other nanosized structures on flat or textured substrate surfaces [7], which use the phenomenon of self-assembling of such structures under the influence of surface relief. We have reported on application of (100) In₄Se₃ surface as template for directed self-assembly fabrication of 1D indium nanostructures array yet [8, 9].

This paper focuses on the method of obtaining metallic indium ordered nanostructures on the (0001) surface of layered semiconductor InSe single crystals, based on the self-assembling effect due to the crystallographic structure of InSe (0001) surface as template.

2. EXPERIMENTAL

InSe layered semiconductor crystals have been grown by Bridgman–Stockbarger method from previously synthesized In–Se melts, which have homogeneous structure. The synthesis was carried out to obtain non-stoichiometric melt with 48 at.% of Se, that allowed high-quality InSe crystals to be grown [10]. Data on electron mobility show value 2000 cm²/V·m at 200 K and photo excited carriers' lifetime value for carrier drift along the layer plane is approximately 0.3 ms that also verify high structural perfection of grown InSe crystals. Samples for STM/STS studies had special 3×4×6 mm³ shape for cleavage *in situ*. Thus, the several cleavages could be obtained for structurally perfect InSe samples in UHV. InSe samples were cleaved by stainless tip *in situ* and just obtained (0001) surface plane was studied by STM/STS. It should be noted, that even despite of the low adsorption capacity of the InSe surfaces, which is confirmed by the history of many studies [11], including ours [12], even in UHV, it is necessary to take into account the possibility of the influence of the atmosphere of residual gases on the formation of surface nanostructures.

STM/STS data were obtained by Omicron Nano Technology STM/AFM System operating with UHV better than 10^{−10} Torr at room temperature. The acquisition of STM data was conducted in the constant current mode. Free software WS&M v.4.0 from Nanotec Electronica [13] was used while analysing and processing of STM data. Low energy electron data (LEED) were acquired by ErLEED 100 optics de-

signed by SPECS Surface Nano Analysis GmbH.

Thermal evaporator EFM-3 was applied for indium deposition *in situ*. Indium ion current inside the effusion cell was maintained to be constant during the indium deposition. The deposition rate was kept at approximately 0.07 mL/min. Small deposition rates were chosen intentionally to produce hetero growth, rather than obtaining of polycrystalline films at high deposition rates. Such rates allowed organizing an activation-migration movement of deposited indium with localization on growth activation centres under consequent annealing at 500 K during 3–5 min.

3. RESULTS AND DISCUSSION

The possible application of InSe (0001) surface as template for indium deposited nanosystem formation causes preliminary detailed analysis of the topology of the substrate. The initial InSe cleavage surfaces topology was studied with nanoscale resolution by STM technique. Figs. 1, *a*, *b* show surface topology of $22 \times 22 \text{ nm}^2$ image and its 2D Fast Fourier Transform (FFT) filter revealing hexagonal ordering of surface structure. Typical experimental dataset contains 400×400 acquisition points. Thus, STM data spatial resolution in this case, is determined only by the physical limitations of the STM method, *i.e.*, $\sim 1 \text{ \AA}$. Fig. 1, *c* shows enlarged fragment of above filtered image with measured hexagonal surface lattice constant equal to 4 \AA as derived from height profile on Fig. 1, *d*. The similar values were calculated from LEED experimental data shown on Fig. 1 *e*, *f*. Such derived values correlates well with the same for the bulk InSe [14].

The LEED pattern, shown in Fig. 1, *e*, shows sharp spots arranged in hexagonal manner of the 1st, 2nd and even 3rd orders, consequently indicating outstanding (0001) InSe surface crystalline quality on macro scale. Acquired LEED clear spot patterns reveal the presence of large-scale flat terraces, which extend up to hundreds of microns along the surface. This conclusion can be drawn from the fact that the primary electron beam spot has a diameter up to 1 mm.

However, LEED data on Fig. 1, *f* also confirms that (0001) InSe surface isn't flat in nanoscale. It's well known [11], that InSe crystal layer-packet are characterized by the 'sandwich' pattern in which two inner sublayers of In atoms are located between the two outer sublayers of the Se atoms. For low-energy electrons, even a small height differences (3D displacement) in surface topography will cause a significant phase shift and noticeable changes in interference pattern in a first-order LEED spots. Thus, hexagonal surface lattice structure of InSe can be represented by a superposition of two 'triangles', one of which is associated with three Se atoms in the outer sublayer, and the other with three In atoms in the inner sublayer of the InSe crystal layer-

packet.

With the growth of the energy of incident electrons, there is a decrease in the intensity of the spots that appear to be the vertices of one of the 'triangles' with the simultaneous preservation/intensification of the spots intensity forming the other 'triangle' (Fig. 1, *f*). Thus, (0001) InSe surface potentially could be used as template in the process of formation of nanostructures that is covered with array of triangular

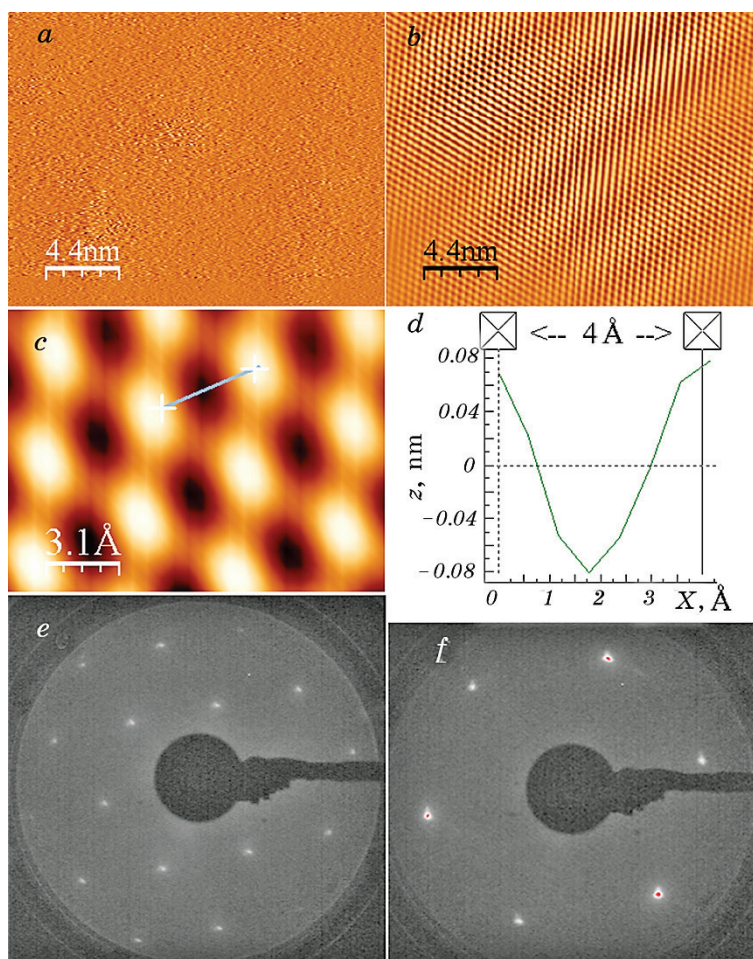


Fig. 1. High resolution STM image of (0001) InSe UHV cleavage: 2D 22×22 nm² image, +1.5 bias, 253 pA tunneling current (*a*); 2D FFT filtered image (*b*); 1.1×1.48 nm² zoomed area from (*b*) 2D FFT filter with hexagonal surface lattice with 4 Å parameter as derived from topographical profile on (*d*) (*c*); LEED patterns of the as-cleaved sample of InSe, acquired at a primary electron energy of 125 eV and 45 eV (*e*, *f*), respectively.

shaped cites.

Technologies for the formation of metallic nanostructures on the naturally or intentionally, *e.g.*, by mechanical influence, lithography *etc.*, textured surfaces often use a vapour phase–a liquid phase–solid phase or vapour phase–solid phase–solid phase methods [7]. These methods are based on the effect of the thin metal films transformation, deposited on the surface of substrate, under the action of elevated temperatures into nanosized droplets. Since, this process is opposite to the phenomenon of surface wetting, it is called the dewetting one. Thus, solid-state dewetting offers a straightforward fabrication route for substrate-supported metal nanostructures.

This effect is caused by minimizing the energy of the deposited coating–substrate system relating to the phase interaction of the metal and the substrate, as well as the free surface energy of both phases of the metal and the substrate. A metal coating deposited at room temperature exists in a thermodynamically unfavourable state, that is, metal atoms on the surface lack the kinetic energy needed to reorganize deposit into an energy-efficient state. Thus, during the heating of the substrate with deposited metal, an energy-efficient conversion of a metal deposited coverage with a large free surface energy into three-dimensional droplets is realized to reduce the overall ratio of the surface area to the volume.

It looks like, that surfaces of 2D layered crystals are one among most perspective templates for above mentioned procedure. From a physical point of view, it is clear that effective pattern assembly requires nanostructure precursor's mobility over the substrate surface, a property that is naturally connected with poor adhesion. Because of intrinsic nature of van der Waals interlayer bonding, InSe layered crystal possesses relatively good ambient stability [11, 12], thus it has excel-

TABLE 1. Kinetics of surface roughness parameters for In/(0001)InSe nanosystem.

Parameters Curve on Fig. 2	RMS, nm	Skewness	Kurtosis	Sample state
1	0.0988	0.5265	3.8672	Initial
2	0.0596	3.624	57.2702	25 s deposition
3	0.0678	0.3998	8.2953	65 s deposition
4	0.0907	0.0171	8.4755	95 s deposition
5	0.0448	0.9924	20.8569	Annealed at 200°C
6	0.1431	0.3463	2.9604	335 deposition

lent prospects to be applied as template for solid-state dewetting formation of metal-semiconductor nanosystems.

We analysed the kinetics of formation of the indium deposit—InSe surface nanosystem using STM data acquired over the large surface areas using the Roughness Analysis tool in WSxM application. Fig. 2 shows results of statistical analysis in height distribution of pixels over $1 \times 1 \mu\text{m}^2$ areas for initial, deposited and annealed surfaces. Table 1 shows kinetics of surface parameters of In/(0001) InSe nanosystem derived from roughness analysis and their correlation with curves on Fig. 2. InSe (0001) surface before deposition (see Fig. 2, curve 1) shows almost Gaussian distribution in height distribution of STM image (kurtosis parameter (peakness) equal to 3.0 is characteristic for Gaussian distribution). Indium deposition (see Fig. 2, curve 2) leads to increase of surface asymmetry (symmetry of surface's pixels distribution is characterized by skewness parameter equal to zero, values above it shows on peaks and below on holes) with appearance of substantial peaks up to two indium atoms diameter in height, when considering indium covalent radius 1.42 \AA . However, in this case the surface can be considered as almost smooth crystal terrace with the presence of a relatively small number of deposited indium peaks, as can be seen from the distribution of pixels' heights (see Fig. 2, curve 2). Further indium depositions (curves 3, 4) lead to decrease of surface peakness, apparently, due to the smoothing of the STM studied surface caused by indium deposition and the formation of a 'new surface', *i.e.*, covered by indium. Annealing, in fact, restores the peakness of the surface (see Fig. 2, curve 5 and the corresponding parameters in the Table 1), but in the

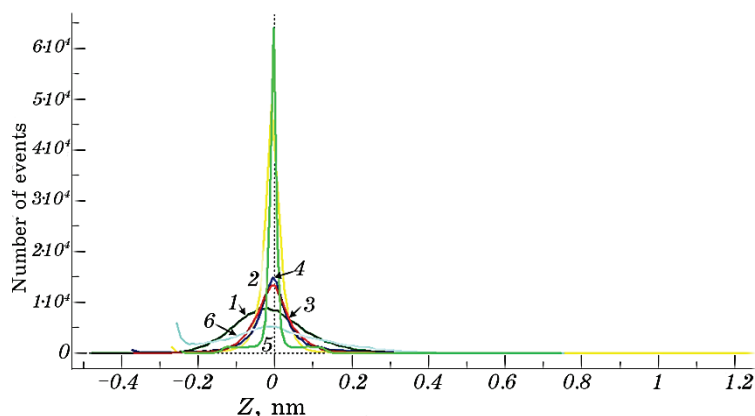


Fig. 2. Height distribution of pixels for $1 \times 1 \mu\text{m}^2$ STM images on (0001) InSe surface before and after indium deposition: 1—initial, 2—25 s deposition, 3—65 s deposition, 4—95 s deposition, 5—annealed (200°C), 6—335 s deposition.

specific manner. The further high resolution STM results on Figs. 3, 4 show that the newly formed nanostructures are characterized by a specific symmetry.

In this case, the topography of InSe surface plays a decisive role in activating the effect of self-organizing nanostructures in the directional technique of their assembly, in such a way that the formation of nanostructures is determined by conditions of hexagonal symmetry, which characterizes the (0001) InSe surface. Evidently, that geometrically heterogeneous (in height) (0001) InSe surface is used to activate the dewetting phenomenon in a manner that leads not only to the formation of triangular shaped nucleus of deposited indium nanostructures (see Fig. 3), but also forces the assembly to occur even in macroscale (see Fig. 4) in a highly deterministic manner.

Figure 3 shows triangular shaped nanostructures and their derived from topographical profile equilateral size of 10 nm. The obtaining of

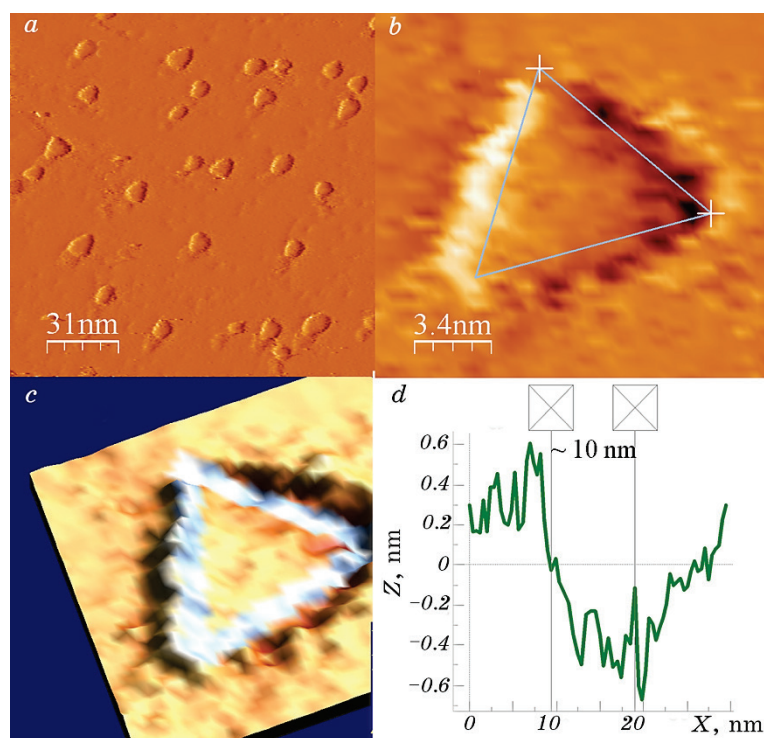


Fig. 3. STM study of In/(0001)InSe nanosystem surface after 95 s In deposition subsequently annealed (200°C): 2D image 160×160 nm², +1.5 V bias, 103 pA tunneling current (*a*); 2D 16×16.7 nm² image of zoomed triangular shape nanostructure and its 3D image (*c*) (*b*); subsequent topographical profile deriving size of triangular indium induced nanostructure (*d*).

nanostructures with geometric sizes that are different from the period of the hexagonal crystallographic structure (crystallographic parameter $a = 4 \text{ \AA}$) on the surface (0001) of the InSe crystal, acting as a directed template for their formation, is based on the known Gibbs–Thomson effect, which has a significant influence on the growth of nanostructures: at a given vapour pressure, smaller deposited particles of indium desorb more atoms than larger, which stops the growth of nanostructures from particles smaller than a certain critical radius [15].

Figure 4, *a* shows sufficiently large in macro scale typical STM image of In/InSe nanosystem surface with deposited indium coverage subsequently annealed to activate dewetting process. 2D FFT filter applied to this image presented on Fig. 4, *b* and, especially, its enlarged fragment (see Fig. 4, *c*) allow to conclude about hexagonal ordering of

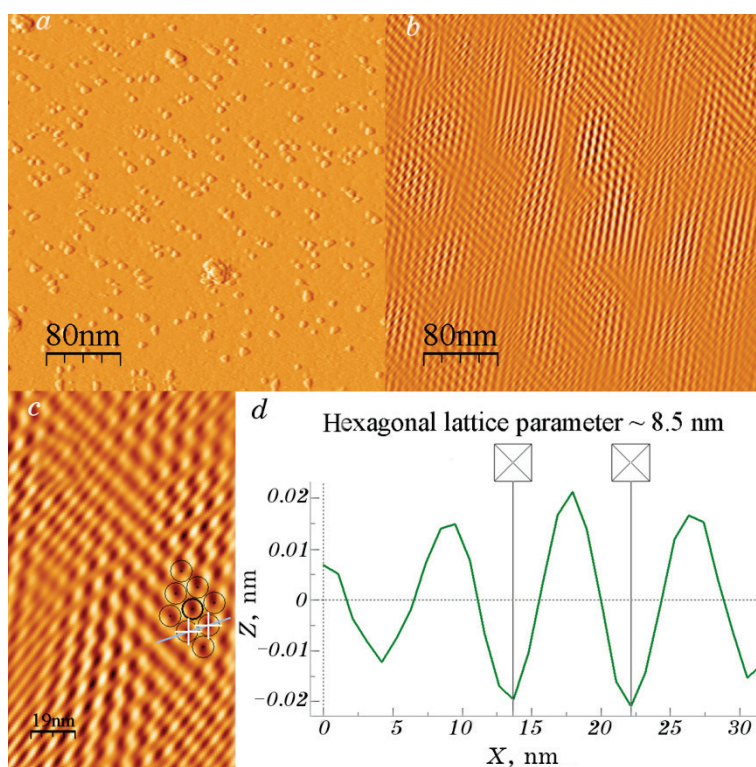


Fig. 4. STM study of In/ (0001) InSe nanosystem surface after 95 s In deposition subsequently annealed (200°C): 2D 400×400 nm² image, +1.6 V bias, 103 pA tunneling current (*a*); 2D FFT filtered image (*b*); 156×94 nm² zoomed area from (*b*) 2D FFT filter with hexagonal lattice model (black circles) (*c*); profile with derived hexagonal surface lattice parameter in the array of nanostructures (*d*).

formed indium nanostructures which corresponds to substrate symmetry. Fig. 4, *c* shows black rings stacked in hexagonal shaped manner overlaid on the STM image of In/InSe nanosystem. This model design fits well to the corresponding image when taking the hexagonal lattice parameter equal to 8.5 nm.

It should be noted that the subsequent deposition of indium leads to the formation of the surface of the In/InSe nanosystem, which, according to the STM data (see Fig. 2, curve 6 and roughness parameters in Table 1), is smoother than the original surface of the crystal in a macro scale. Thus, it can be assumed that a homogeneous, sufficiently thick layer of deposited indium is formed that doesn't 'feel' the InSe substrate topology. Moreover, the subsequent annealing of such In/InSe system in order to activate dewetting process, doesn't lead to the formation of nanostructures clearly shaped and ordered into arrays as described above.

4. CONCLUSIONS

Our work revealed the ability to organize the directed assembly process for a given lattice texture of (0001) InSe cleavage surface. In fact the approach of templated dewetting leads to formation of deposited indium nanostructures the shape and arrangement of which are powered by hexagonal lattice symmetry of surface lattice.

In our opinion, the choice of experimental conditions which are successful for the formations of as shown nanostructures depends on the rate of indium deposition, and consequently, the degree of surface coating by deposit, as well as the choice of heating conditions to activate the dewetting process, is another factor important for the successful formation of indium nanostructures on 2D surfaces of a layered crystal. Given the possible application of InSe layered semiconductor crystals for superfast electronics, this opens new opportunities for creating new functional devices on their basis.

REFERENCES

1. L. Yu. Kharkhalis, K. E. Glukhov, and M. Sznajder, *Acta Phys. Polonica A*, **126** (5): 1146 (2014).
2. A. Politano, D. Campi, M. Cattelan, I. Ben Amara, S. Jaziri, A. Mazzotti, A. Barinov, B. Gürbulak, S. Duman, S. Agnoli, L. S. Caputi, G. Granozzi, and A. Cupolillo, *Scientific Reports*, **7**: 3445 (11pp) (2017).
3. D. A. Bandurin, A. V. Tyurnina, G. L. Yu, A. Mishchenko, V. Zylyomi, S. V. Morozov, R. K. Kumar, R. V. Gorbachev, Z. R. Kudrynskyi, S. Pezzini, Z. D. Kovalyuk, U. Zeitler, K. S. Novoselov, A. Patané, L. Eaves, I. V. Grigorieva, V. I. Fal'ko, A. K. Geim, and Y. Cao, *Nat. Nanotechnol.*, **12**: 223 (2017).

4. P. V. Galiy, T. M. Nenchuk, A. Ciszewski, P. Mazur, I. R. Yarovets', and O. R. Dveriy, *Metallofiz. Noveishie Tekhnol.*, **39**, No. 7: 995 (2017).
5. T. Komesu, H. Yi, S. Gilbert, K. Fukutani, A. J. Yost, A. Lipatov, A. Sinitskii, Ya.B. Losovyj, P. Galiy, J. Avila, C. Chen, M. C. Asensio, and P. A. Dowben, *Symp. F: Surfaces and Interfaces in Multilayered Thin Films and Nano-Composites (E-MRS 2018) (September 17–19, 2018, Warsaw)*, p. F.5.1.
6. J.-S. Rhyee, K. H. Lee, S. M. Lee, E. Cho, S. I. Kim, E. Lee, Y. S. Kwon, J. H. Shim, and G. Kotliar, *Nature*, **459**: 965 (2009).
7. R. A. Hughes, E. Menumorov, and S. Neretina, *Nanotechnology*, **28**: 282002 (24pp) (2017).
8. P. Galiy, P. Mazur, A. Ciszewski, T. Nenchuk, and I. Yarovets, *Eur. Phys. J. Plus*, **134**: 70 (2019).
9. P. V. Galiy, T. M. Nenchuk, P. Mazur, A. Ciszewski, and I. R. Yarovets, *Molecular Crystals and Liquid Crystals*, **674**, Iss. 1: 11 (2018).
10. K. Imai, K. Suzuki, T. Haga, Y. Hasegawa, and Y. Abe, *J. Crystal Growth*, **54**, No. 3: 501 (1981).
11. D. W. Boukhvalov, B. Gürbulak, S. Duman, L. Wang, A. Politano, L. S. Caputi, G. Chiarello, and A. Cupolillo, *Nanomaterials (Basel)*, **7**, No. 11: E372 (2017).
12. P. V. Galiy, T. M. Nenchuk, and J. M. Stakhira, *J. Phys. D: Appl. Phys.*, **34**, No. 1: 18 (2001).
13. I. Horcas, R. Fernandez, J. M. Gomez-Rodriguez, J. Colchero, J. Gomez-Herrero, and A. M. Baro, *Rev. Sci. Instrum.*, **78**: 013705 (2007).
14. D. M. Bercha, K. Z. Rushchanskii, L. Yu. Kharkhalis, and M. Sznajder, *Condensed Matter Physics*, **3**, No. 4: 749 (2000).
15. V. G. Dubrovskii, *Nucleation Theory and Growth of Nanostructures* (Berlin: Springer-Verlag Berlin Heidelberg: 2014).